Scaling laws and minimum threshold currents for quantum-confined semiconductor lasers

Amnon Yariv
California Institute of Technology, Pasadena, California 91125

(Received 3 May 1988; accepted for publication 11 July 1988)

Basic scaling laws are derived for bulk, two-dimensional (quantum well) and one-dimensional (quantum wire) semiconductor lasers. Starting from quantum derivation of the optical properties of confined carriers, the dimensional dependencies of the scaling laws are made explicit. Threshold currents of ~ 100 and 2–3 μA are predicted for single quantum well and quantum wire lasers, respectively. The basic considerations of this analysis were used recently to obtain ultralow threshold quantum well lasers [P. L. Derry, A. Yariv, K. Lau, N. Bar-Chaim, K. Lee, and J. Rosenberg, Appl. Phys. Lett. **50**, 1773 (1987)].

In semiconductor lasers the separate and precise control of electronic (gain) and optical confinement made possible by epitaxial crystal growth and fine lithography make for a rich interplay between "physics" and "geometry"—an interplay which determines the laser threshold. In this letter we show, starting with the fundamental confinement physics, how the threshold currents of conventional bulk (three-dimensional), two-dimensional (quantum well), and one-dimensional (quantum wire) lasers depend on the respective geometrical and physical parameters, and then derive the relevant basic scaling laws for the threshold currents of each class.

The basic generic laser configuration is illustrated in Fig. 1. The active region is a rectangular prism with dimensions $L_z \times L_y \times L$ which is embedded within the optical mode volume $d \times W \times L$. In the case of quantum wells and quantum wires we take the potential well depth as infinite (this puts a limit, in practice, on the smallest well dimensions) and assume that only the first quantized states $(n = 1)$ are involved.

The first major consideration is that of the transparency density. It is defined as the injected carrier density which renders the active region transparent. Clearly, the maintenance of these densities establishes a lower limit on the threshold currents. As an example, we will calculate the transparency density of a quantum wire with equal electron and hole effective masses $(m_e = m_h)$ whose energy diagram is shown in Fig. 2. The transparency condition for an inverted population of Fermions obtains when the condition

$$\hbar\omega = E_{FC} - E_{FV}$$

at the frequency ω of maximum gain, where E_{FC} and E_{FV} are the quasi-Fermi levels for the conduction band and valence band, respectively, since maximum gain is exercised by $\hbar\omega = E_g + (\epsilon_{1,1})_C + (\epsilon_{1,1})_V$. The transparency condition in the case $m_C = m_V$ is obtained when the quasi-Fermi level in the conduction band E_{FC} coincides with the first quantized level $\epsilon_{1,1}$ and E_{FV} with the first quantized level in the valence band. The total number of electrons (or holes) per unit length at transparency is then obtained by integrating the product of the density of states function and the Fermi distribution function from $\epsilon_{1,1}$ to infinity. We neglect contributions from higher subbands which are effectively cut off by the Fermi function:

$$N_{1D}^{tr}\left(\frac{\text{electrons}}{m}\right) = \frac{\sqrt{2m_C}}{\pi\hbar}\int_{\epsilon_{1,1}}^{\infty}\frac{(E_c-\epsilon_{1,1})^{-1/2}}{e^{(E_c-\epsilon_{1,1})/kT}+1}\,dE_c \quad (1)$$

$$= (\sqrt{2m_C}/\pi\hbar)\times 1.072(kT)^{1/2}. \quad (2)$$

The key observation as far as scaling is concerned is that N_{1D}^{tr} is the *lineal* (electrons per unit length) density and that it is *independent* of the cross-sectional dimensions L_z and L_y of the quantum wire. Similar considerations in the case of a quantum well lead to a transparency (area) density

$$N_{2D}^{tr}\left(\frac{\text{electrons}}{m^2}\right) = \frac{m_C}{\pi\hbar^2}\int_{\epsilon_1}^{\infty}\frac{dE_c}{e^{(E_c-\epsilon_1)/kT}+1} = \frac{m_C kT}{\pi\hbar^2}\ln 2, \quad (3)$$

which is independent of the quantum well thickness L_z.

Numerical calculation of the transparency densities using the actual values of m_C and m_V in, say, GaAs, gives values three to four times larger than the values of Eqs. (2) and (3). The transparency requirements[1] can be summarized in

$$N_{3D}^{tr} \sim 1.5\times 10^{18}\ \text{cm}^{-3},$$
$$N_{2D}^{tr} \sim 1.5\times 10^{12}\ \text{cm}^{-2}, \quad (4)$$
$$N_{1D}^{tr} \sim 1.5\times 10^{6}\ \text{cm}^{-1}.$$

The key point to reemphasize is the independence of the above values of N^{tr} of the confinement geometry and the *different* physical dimension of the transparency density in each generic case.

The bulk gains, i.e., gains experienced by a hypothetical optical wave which is completely confined to the active region, can be expressed near the transparency condition by

$$(3D)\,g_{3D} = g'_{3D}(N_{3D} - N_{3D}^{tr}).$$

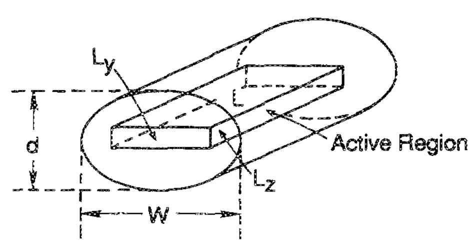

FIG. 1. Basic electron confinement and optical mode geometries.

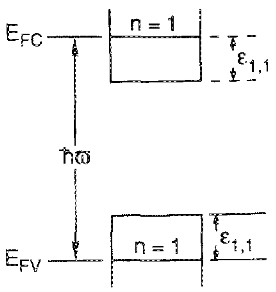

FIG. 2. Energy level diagram of the quantum-confined carriers.

The corresponding expressions for the 2D and 1D cases require some thought. Consider the 2D case. Transparency occurs when $N_{2D} = N_{2D}^{tr}$ (electrons/cm^2). The bulk gain, on the other hand, depends on the *volumetric density* of carriers.[1] We can satisfy both requirements by writing the bulk gain as

$$(2D) g_{2D} = g'_{2D}\left(\frac{N_{2D}}{L_z}\right) - \frac{N_{2D}^{tr}}{L_z}, \qquad (5)$$

where g'_{2D} is a constant. In a similar fashion,

$$(1D) g_{1D} = g'_{2D}\left(\frac{N_{1D}}{L_z L_y} - \frac{N_{1D}^{tr}}{L_z L_y}\right).$$

The g's are constant specific to the material and the dimension of the confinement. They are called the differential gain constant, the differential gain constants, and the explicit dimensional dependencies (i.e., on L_z and L_y) of the three cases follow from basic quantum-induced transition rate considerations. This dependence, as well as those expressed by Eq. (4), is central to what follows.

We will next derive expressions for the threshold current densities for lasers whose modes propagate along the axis x of the active region. First consider the three-dimensional case. The threshold condition is

$$\Gamma g'_{3D}(N - N_{3D}^{tr}) = \Gamma \alpha_{fc} + (1/L)\ln R^{-1} + \alpha_{scatt}, \qquad (6)$$

where $\Gamma \sim L_z/d$ is the optical confinement factor, $\alpha_{fc} = bN_{3D}$ is the bulk free-carrier absorption coefficient of the active region material, and α_{scatt} is the scattering loss of the mode. Solving for N and taking the threshold current as $(N_{3D} e V_a/\tau)$, where $V_a = WL_zL$ is the volume of the active region and τ the carrier lifetime, leads to

$$(I_{th})_{3D}\left(\frac{\eta\tau}{e}\right) = N_{3D}^{tr}(WL_zL) + \left(\frac{Wd}{g'_{3D}}\right)\ln R^{-1} + \frac{(WLd)}{g'_{3D}}\alpha_{scatt}, \qquad (7)$$

where $\eta \equiv 1 - b/g'_{3D}$.

A similar calculation for a quantum well, but taking $\alpha_{fc} = bN_{2D}/L_z$ and, as before $\Gamma = L_z/d$, gives

$$(I_{th})_{2D}\left(\frac{\eta\tau}{e}\right) = N_{2D}^{tr}(WL) + \frac{(Wd)}{g'_{2D}}\ln R^{-1} + \frac{(WLd)}{g'_{2D}}\alpha_{scatt}. \qquad (8)$$

In the quantum wire case we take $\Gamma = L_z L_y/dW$, leading to

$$(I_{th})_{1D}\left(\frac{\eta\tau}{e}\right) = N_{1D}^{tr} L + \frac{(Wd)}{g'_{1D}}\ln R^{-1} + \frac{(WLd)}{g'_{1D}}\alpha_{scatt}. \qquad (9)$$

Equations (7)–(9) are the basic scaling relations for the three generic laser classes. The quantum confinement physics is now represented explicitly by the appropriate geometry-independent transparency densities.

The scaling laws explain some basic observations and act as design guides. For example, in a conventional (three-dimensional) laser the first term on the right side of Eq. (7) dominates, which explains the length (L) and active region thickness (L_z) dependence of I_{th} in such lasers. In the quantum well (two-dimensional) laser for conventional lengths, say $L < 500\,\mu$m, it is the second term on the right side of Eq. (8) which dominates. This explains why the (total) threshold current of high quality material uncoated quantum well lasers is independent of the length L.[2] Since this dominant term can be reduced to near zero with $R \to 1$, we would expect a major reduction of I_{th} as the facet reflectivity is increased. Indeed, the recent demonstration of submilliampere threshold currents exploited exactly this point and values of $R \sim 0.8$ resulted in nearly an order of magnitude lowering of I_{th} (0.55 mA) from those of uncoated lasers ($R \sim 0.31$). The relative insignificance of the second term on the right side in the three-dimensional case Eq. (7) explains why the same strategy does not work in conventional (three-dimensional) lasers. We also note that when, in the process of evaluating intrinsic quantum well material, we compare the threshold current densities (I_{th}/WL) of quantum well lasers made from the material, the dominant second term varies as L^{-1}. The only meaningful comparison is thus of very long lasers and/or lasers with $R \to 1$ where the reflectivity term is negligible. The minimum threshold current density of a quantum well laser in the limit $R \to 1$ and $\alpha_{scatt} = 0$ is

$$\frac{(I_{min})_{2D}}{(WL)} = \frac{N_{2D}^{tr} e}{\tau\eta} \sim 60\ \text{A/cm}^2$$

for $\eta \simeq 1$, $\tau = 4 \times 10^{-9}$ s, and $N_{2D}^{tr} = 1.5 \times 10^{12}$ cm^{-2}. This shows that recently achieved values of 88 A/cm^2 in our laboratory are approaching the theoretical limit. In a practical laser with, say, $W = 1.5\,\mu$m, $L = 120\,\mu$m, the value of the I_{th} comes out to ~ 0.1 mA. We note that the lowest reported result is $I_{th} \sim 0.55$ mA.

In a quantum wire laser the situation is similar to that of a quantum well laser. The second term on the right side of Eq. (9) will dominate unless reduced by allowing $R \to 1$. If we neglect α_{scatt}, then the threshold current of a laser with $R \simeq 1$ and, say, $L = 100\,\mu$m will be

$$(I_{th})_{1D} \sim (N_{1D}^{tr})\frac{eL}{\tau} \sim 0.6\,\mu\text{A},$$

where we use $N_{1D}^{tr} \sim 1.5 \times 10^6$ cm^{-1}, $\eta \approx 1$, and $\tau \sim 4 \times 10^{-9}$ s. Such a laser can only muster a maximum modal gain[3]

$$(\gamma_{max})_{1D} = \frac{\Gamma_z \Gamma_y}{L_z L_y}\frac{k^2\mu^2}{n^2\epsilon_0\hbar^{3/2}}\sqrt{m_r T_2}, \qquad (10)$$

where L_z and L_y are the quantum wire cross-sectional dimension, μ the transition matrix element, Γ_z and Γ_y the optical confinement factors, m_r the reduced mass, and T_2 the carrier dephasing time. Equation (10) leads to a maximum gain $\gamma_{max} \sim 7$ cm^{-1}, which might not be sufficient to overcome losses in pratical lasers. In this case, an array of parallel quantum wires can be used to obtain the needed total gain.

In summary, the basic scaling laws for the threshold current of quantum confined lasers are derived and are used to explain basic observations as well as serve as a guide in designing ultralow threshold lasers. Using the above considerations, we find that threshold currents of 100 μA from present generation quantum well lasers and of 2–3 μA in quantum wire lasers are possible. Further improvements, possibly by a factor of $\sim$4–5, can be anticipated if we succeed in reducing the hole mass in GaAs wells and wires to near that of the electron.

Fruitful discussions with M. Mittelstein and P. Derry are gratefully acknowledged. This work was supported by the Office of Naval Research and the Defense Advanced Research Projects Agency.

[1]Y. Arakawa and A. Yariv, IEEE J. Quantum Electron. **QE-21**, 1666 (1985).
[2]P. S. Zory, A. R. Reisinger, L. J. Mawst, G. Costrini, C. A. Zmudzinski, M. A. Emanuel, M. E. Givens, and J. J. Coleman, Electron. Lett. **22**, 9 (1986); also H. Chen (private communication).
[3]P. L. Derry, A. Yariv, K. Lau, N. Bar-Chaim, K. Lee, and J. Rosenberg, Appl. Phys. Lett. **50**, 1773 (1987); also K. Lau, P. L. Derry, and A. Yariv, Appl. Phys. Lett. **52**, 88 (1988).